Rabi oscillations and rapid-passage effects in the molecular-beam CO_2-laser Stark spectroscopy of CH_3F

A. G. Adam, T. E. Gough, N. R. Isenor, and G. Scoles
Centre for Molecular Beams and Laser Chemistry, University of Waterloo, Waterloo, Ontario, Canada N2L 3G1
(Received 12 April 1985)

Sub-Doppler molecular-beam laser Stark spectroscopy has been employed to produce high-contrast Rabi oscillations in the ν_3 band of CH_3F. By varying the intensity of the cw CO_2 laser, up to five complete oscillations were observed before the phenomenon was washed out by rapid-passage effects and damping mechanisms. Besides being useful in clarifying key features of coherent ir molecular-beam spectroscopy, the observation of Rabi oscillations provides one of the most accurate means of directly measuring transition dipole moments. Analysis of the present data on three rovibrational transitions, $Q(1,1)\ -1\leftarrow 0$, $P(1,0)\ 0\leftarrow 0$, and $R(1,1)\ 0\leftarrow 1$, has yielded a rotationless transition dipole moment of 0.21 ± 0.01 D for the $\nu_3=1\leftarrow 0$ vibration. This result is in agreement with values estimated from both band-intensity and absorption-coefficient data in the literature.

INTRODUCTION

Rabi oscillations in the infrared have been observed only very recently[1] and require sub-Doppler resolution which can be achieved by crossing a supersonic molecular beam with a stabilized laser beam. The narrow velocity distribution of the supersonic beam ensures a narrow distribution of the molecule-laser interaction times which is essential to the observation of a well-defined Rabi angle. Also the plane phase fronts of the TEM_{00} laser beam are required to avoid frequency sweeps (as encountered by the moving molecule) which may give rise to inversion[1] instead of Rabi oscillations. Although well-defined Rabi oscillations are not essential to the observation of Ramsey fringes, a system capable of producing them is desirable for simple modeling of the latter phenomenon beyond the low-power regime. A proper understanding of the dynamics of the molecular interaction with the laser field in one crossing is a prerequisite to understanding the dynamics in two or more interactions. The separated-field method of producing Ramsey fringes allows for large improvements in resolution[2–5] which are unobtainable in a single crossing because of transit-time broadening. This work is therefore relevant to linewidth determinations and frequency-standard applications. The observation of Rabi oscillations also provides one of the most accurate means of gauging transition dipole moments and thereby determining excited-state lifetimes. The transition moment can be determined directly from the field and interaction time required for the system to evolve through a certain Rabi angle.

The molecule chosen for the present study is fluoromethane (CH_3F), which may be considered the "workhorse" of CO_2-laser spectroscopy. Its ir spectrum is well understood[6] and the low J,K states into which the population is readily concentrated in a supersonic beam[7] are easily Stark tuned into resonance with CO_2-laser lines. Rabi oscillations and Ramsey fringes have been observed[1,5] with SF_6 under crossed molecular-beam—laser-beam conditions, where the experiments depended upon the almost exact coincidence between a certain molecular transition and a CO_2-laser line. By using the laser Stark method the number of accessible transitions is greatly increased and the ease with which a spectral profile of a line can be scanned outweighs any experimental disadvantages, principally electric field nonuniformities, introduced by the Stark electrodes. In addition the successful application of the technique to CH_3F with the resulting Rabi oscillations means that other Stark-tunable molecules, such as NH_3, CH_3Br, and CH_3Cl, may be similarly investigated in the future.

THEORY

The Bloch-equation formulation[8] may be used to describe the interaction of the laser beam with the molecules involved in this experiment since the two levels coupled by the laser radiation form an isolated two-level system. If we neglect excited-state decay (a lower limit for the upper-state lifetime is ~ 20 ms, estimated from the vibrational transition moment, which is large when compared to the molecular transit time through the laser field of $\sim 4\ \mu$s) and assume no dephasing due to Stark-field inhomogeneities and molecule-molecule interactions, the optical Bloch equations simplify to

$$\dot{\mathbf{R}}=\mathbf{R}\times\boldsymbol{\beta}\ , \tag{1}$$

where the unit vector $\mathbf{R}$ describes the state of the two-level system and $\boldsymbol{\beta}$ is the vector driving $\mathbf{R}$, which is defined as

$$\boldsymbol{\beta}=\frac{\mu\mathscr{E}}{\hbar}\hat{1}-(\omega-\omega_l)\hat{3}\ , \tag{2}$$

where μ is the transition dipole moment, $\mathscr{E}$ the laser-field amplitude, ω the transition frequency, and ω_l the laser frequency (rad/s). The unit-vector notation refers to the orthogonal Cartesian axes of the space in which $\mathbf{R}$ moves, that is, a frame rotating at the laser frequency ω_l.

The components of $\mathbf{R}$ are determined by the following:

$$\dot{R}_1 = -(\omega-\omega_l)R_2 \,, \tag{3a}$$

$$\dot{R}_2 = (\omega-\omega_l)R_1 + \frac{\mu\mathscr{E}}{\hbar}R_3 \,, \tag{3b}$$

and

$$\dot{R}_3 = -\frac{\mu\mathscr{E}}{\hbar}R_2 \,. \tag{3c}$$

The quantity $\mu\mathscr{E}/\hbar$ is the Rabi frequency[9] and in the absence of relaxation and detuning is the angular frequency at which the molecular state oscillates between the pure lower and upper states for constant $\mathscr{E}$. In the case of a molecular beam passing through a TEM_{00} laser beam, the equations must be numerically integrated over the Gaussian-field profile. In performing this integration it has been found useful to use the analytic solution to the coupled equations[10] that has been derived for a constant β. This solution was used to calculate the new **R** vector positions for the small integration steps over the Gaussian profile.

For the special case of zero detuning, $\omega-\omega_l=0$, we may obtain, very simply, an experimental value of the transition dipole moment. The solutions of the component Bloch equations become

$$R_1(t)=0 \,, \tag{4a}$$

$$R_2(t)=\sin\left[\frac{\mu}{\hbar}\int_{-\infty}^{t}\mathscr{E}(t')dt'\right] , \tag{4b}$$

and

$$R_3(t)=-\cos\left[\frac{\mu}{\hbar}\int_{-\infty}^{t}\mathscr{E}(t')dt'\right] . \tag{4c}$$

After a complete transit of the laser beam, the value of R_3 is

$$R_3(\infty)=-\cos\left[\frac{\mu}{\hbar}(\mathscr{E}t)_{\text{eff}}\right] , \tag{5}$$

where the value of $(\mathscr{E}t)_{\text{eff}}$ is given by

$$(\mathscr{E}t)_{\text{eff}}=\frac{2}{v}\left[\frac{P}{c\epsilon_0}\right]^{1/2} , \tag{6}$$

with v being the molecular speed and P the power in the polarization component of the laser beam effective for the transition. Equation (6) was derived using a Gaussian-intensity profile and the Poynting vector and is independent of the laser spot size w_0. The energy deposited in the system, after laser excitation is $\frac{1}{2}\hbar\omega[1+R_3(\infty)]$. Thus the detector signal is proportional to $1+R_3(\infty)$. If we plot this signal versus $P^{1/2}$ and fit the function $1-\cos\theta$ to the plot, we obtain, very simply, a value for the transition dipole moment μ.

Damping mechanisms that wash out the Rabi oscillations may be introduced very easily into the Bloch formalism. In particular the frequency sweeps expected due to wave-front curvature[11] and Stark-field inhomogeneities may be added by modifying Eq. (2). A frequency-sweep term, given by the rate of change of the laser-field phase as seen by the molecule, need only be added to the $\hat{3}$ component of β in order to predict wave-front curvature effects. Similarly a term representing a frequency sweep due to a changing Stark field in the direction of motion of the molecules may be added to predict electric field effects.

EXPERIMENT

The supersonic molecular beam was formed by seeding 1 vol% CH_3F in He gas and expanding the mixture through a 35-μm-diam nozzle. The nozzle was located 1.0 cm from a 300-μm-diam skimmer, which together with a 350-μm-wide collimating slit located 65 cm from the skimmer, defined the horizontal profile of the molecular beam. The vertical profile was defined by the skimmer and the 6-mm height of the detector. A schematic view of the apparatus is shown in Fig. 1. The speed of the CH_3F molecules in the beam was determined by Doppler-shift measurements to be 1590 m/s with a half width at half maximum (HWHM) of 50 m/s for a nozzle stagnation pressure of $\simeq$450 kPa. The beam was detected by a liquid-He-cooled germanium bolometer (Infrared Laboratories Inc.), which has a responsivity of 1.1×10^6 V/W and a noise equivalent power (NEP) of 3.4×10^{-14} W/Hz$^{1/2}$ at 75 Hz. The bolometer, which was located 70 cm from the skimmer was used to detect the kinetic energy, internal energy, and energy of condensation of the molecules as a dc signal. In order to obtain spectra, the laser beam was chopped to allow phase-sensitive detection of the internal energy change of the molecules due to absorption of energy from the CO_2 laser.

The Stark field was produced by two circular stainless-steel plates 10.0 cm in diameter with a spacing of $\simeq$5.4 mm. Both plates were lapped to a flatness of $\leq$0.1 μm, and one of them was provided with two torsional pivots. The flatness of the surface and the capability of tilting one plate about two orthogonal axes, one parallel to the laser beam and the other to the molecular beam, allowed a good degree of parallelism to be obtained. The $Q(1,1)$ transition of interest could be observed with only a few kilovolts applied across the plates, a factor that is important in connection with line broadening due to field inho-

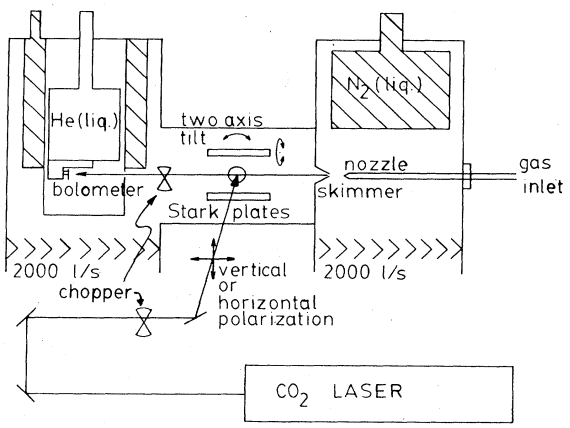

FIG. 1. Schematic view of the apparatus.

mogeneities. A ramping Stark voltage was used to scan the region of interest. rf modulation superimposed on the dc Stark voltage could be used to produce satellites of the parent line shifted by the modulation frequency. These satellites were used to obtain frequency calibration for a Stark scan and allowed for the easy determination of transition linewidths.

There are three main contributions to the linewidths: transit-time broadening, residual Doppler width, and electric field inhomogeneities. Transit-time broadening was calculated to be $\simeq$180 kHz full width at half maximum (FWHM) using a $1/e$ spot size of $w_0=3.29$ mm for the laser. The residual Doppler full width due to molecular-beam divergence was calculated to be $\lesssim$160 kHz. These two values combined in quadrature were enough to account for the best observed $Q(1,1)$ transition linewidth of $\simeq$215 kHz showing that electric field inhomogeneities at the low Stark voltage needed for this transition have minimal influence. Calculations based on a uniform charge distribution over the parallel plate configuration used indicate that the field homogeneity is ~ 1 part in 10^5, which corresponds to a broadening of $\simeq$20 kHz for the $Q(1,1)$ transition.[12] The result in Ref. 13 indicates that the field is probably even more homogeneous so one part in 10^5 can be taken as an upper limit for the inhomogeneity.

The line-tunable CO_2 laser was stabilized by servolocking to an external cavity. The cavity itself was servolocked to a stabilized He-Ne laser to eliminate effects due to room-temperature drifts. While the details of the laser stabilization system will be reported elsewhere, the fact that by using the separated-field technique,[14] linewidths as low as 150 kHz have been observed indicates that the laser is presumably stable to much better than this and therefore its stability does not play a role in the broadening of the spectral lines. A partially transmitting ZnSe lens was used as a laser output coupler in order to produce a beam waist external to the laser. The waist was calculated to be $\simeq$1.60 m from the output coupler with a $1/e$ field radius of $\simeq$3.29 mm. The confocal parameter[15] at the $9P(18)$ CO_2 transition frequency used for the $Q(1,1)$ $-1\leftarrow 0$ transition was therefore $\simeq$3.5 m. A II-VI PAZ-10-AC zinc selenide polarization rotator-attenuator was used to control the polarization and the power of the laser entering the interaction region.

DATA AND ANALYSIS

Spectra of the $R(1,1)$ $0\leftarrow 1$, $Q(1,1)$ $-1\leftarrow 0$, and $P(1,0)$ $0\leftarrow 0$ transitions were observed for different values of the laser power. Rabi oscillations were obtained from this data by plotting the bolometer signal at line center against the square root of the laser power polarized perpendicular or parallel to the Stark field depending on the type of transition excited. Because the $Q(1,1)$, $-1\leftarrow 0$ transition had the lowest Stark voltage and therefore fewer electric field homogeneity problems, it was used to study how best to achieve Rabi oscillations and to observe the effects of different damping mechanisms on the oscillations. Figure 2(a) shows the $Q(1,1)$ Rabi oscillation obtained with the laser beam crossing the molecular beam $\simeq$1.60 m from the laser. Five complete oscillations are apparent in this data with a contrast of $\simeq$94% between the first maximum and the first minimum. Data obtained at a distance of 2.45 m, 85 cm away from the beam waist, are shown in Fig. 2(b). The contrast is still very good ($\simeq$90%) but the signal shows a definite upward trend at the higher laser powers. In both cases, great care was taken to ensure orthogonality of the beam crossing by minimizing the linewidth, a condition that also maximized oscillation contrast. These data clearly show that the position of the beam waist on the molecular beam that was so critical in earlier results[1] on SF_6 is not a problem in the present experimental set up probably because of the much larger confocal parameter associated with our laser.

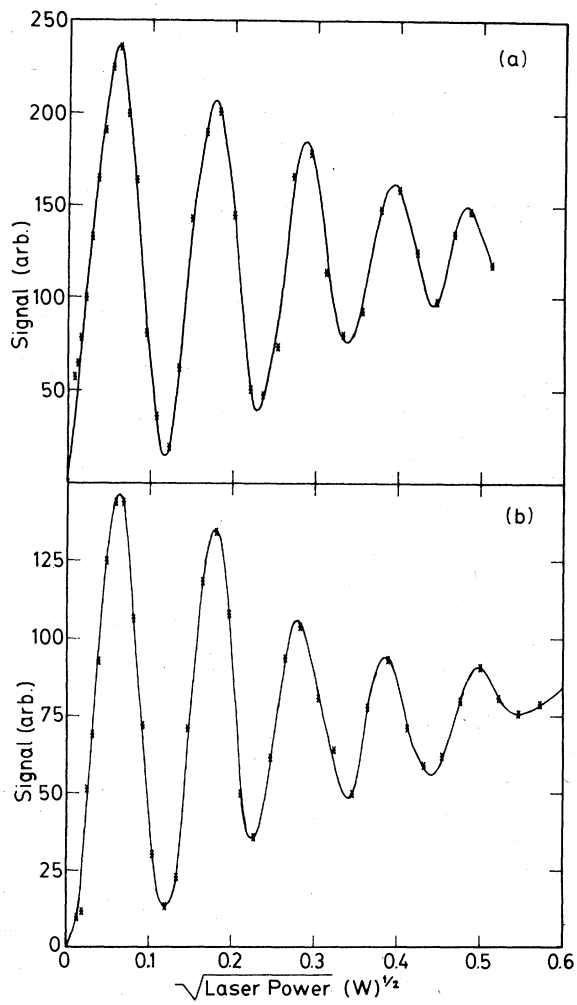

FIG. 2. Rabi oscillations observed for the $Q(1,1)$ $-1\leftarrow 0$ transition. The laser waist is located on the molecular beam for the data in (a) and 85 cm off the molecular beam for the data in (b). The FWHM linewidth for this transition is $\simeq$215 kHz.

The effects of Stark-field homogeneity were studied by tilting the adjustable plate (see Fig. 1) about two orthogonal axes corresponding approximately to the directions of the two beams. At the laser-beam waist position, the plate was tilted about the laser-beam axis to achieve the results

of Figs. 3(a) and 3(b). Tilting the plate had the effect of increasing the linewidth at low laser power, and as well to yield inversion of the population for larger laser fields. To a good approximation, tilting the plate in this direction causes the molecular transition frequency to sweep linearly with time as the molecule traverses the laser beam. This causes a rapid-passage-like effect that leads to inversion. The data show that an increase of about 200 kHz in linewidth from the electric field inhomogeneity is enough to almost completely damp out the Rabi oscillations and invert the population. The Stark plate was also tilted about the molecular-beam direction and the resulting data indicated that inversion and damping were also obtained in this case. Inversion, however, was not expected. This result is probably because the tilt adjustment about the molecular-beam axis is much coarser than the adjustment about the laser axis and the two motions are not perfectly orthogonal. A movement of the coarse adjustment therefore may give a small movement in the other direction that is enough to produce the rapid-passage phenomenon.

The Rabi oscillations obtained for the $R(1,1)$ $0\leftarrow 1$ and $P(1,0)$ $0\leftarrow 0$ transitions are shown in Fig. 4 for comparison with the $Q(1,1)$ $-1\leftarrow 0$ Rabi oscillation data of Fig. 2(a). Each transition has a distinctly different oscillation frequency. The three sets of data were fitted with a damped cosine function to determine the periods of oscillation in terms of the square root of the laser power [see Eqs. (5) and (6)]. From the fits, transition dipole moments of 0.028, 0.065, and 0.123 D were obtained for the $R(1,1)$, $Q(1,1)$, and $P(1,0)$ transitions, respectively. The error on these values for the transition moment is mainly due to the accuracy of the polarization rotator-attenuator used to control the laser power. The attenuator that uses rotation of stacked Brewster plates to control polarization and power had angular divisions of 2° and resettability of only ±1°. Furthermore, thermal effects caused small changes in the transmitted laser power and therefore gave

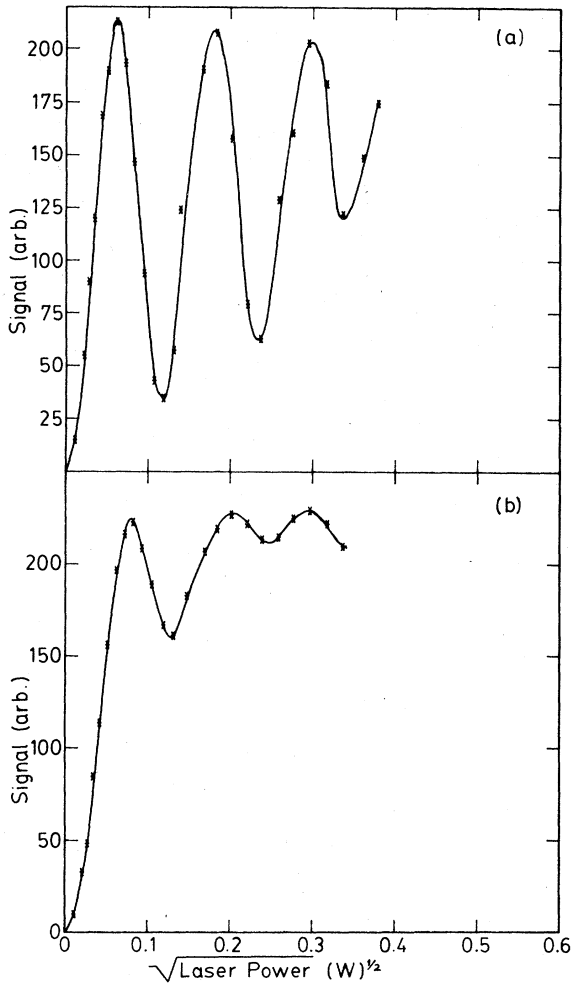

FIG. 3. Effect of Stark-field homogeneity on the Rabi oscillations is shown. The measured FWHM linewidth of the data in (a) is 232 kHz while the linewidth is 414 kHz for (b). These linewidths correspond to tilts of 0.033 and 0.130 mrad of the Stark plate, respectively. The laser waist was located on the molecular beam for these data.

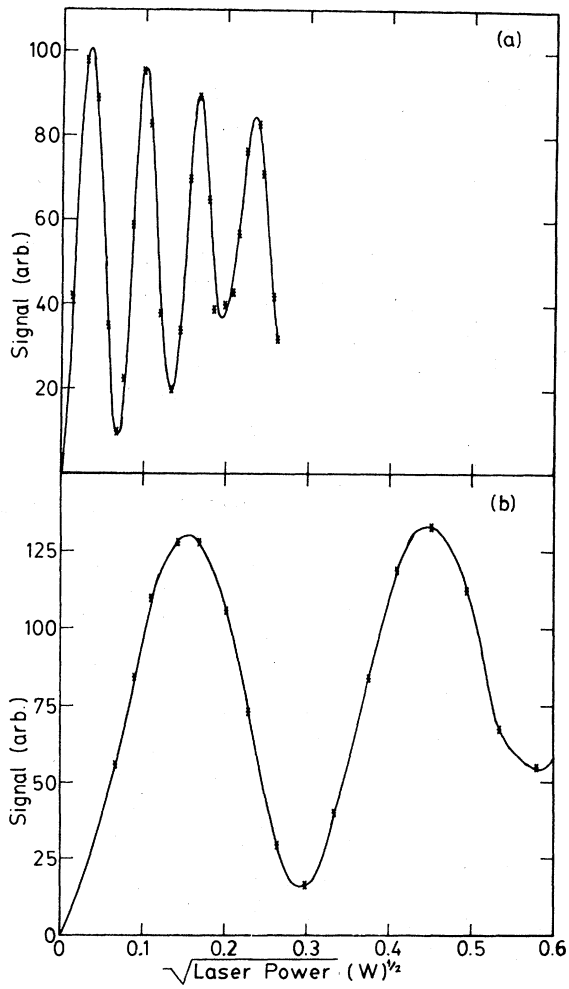

FIG. 4. Observed Rabi oscillations for the $P(1,0)$ $0\leftarrow 0$ transition (a) and the $R(1,1)$ $0\leftarrow 1$ transition (b).

a zero wander. In addition to the zero correction of the attenuator, the observed transition moments must be corrected for molecular rotation[16] before the pure $\nu_3=1\leftarrow 0$ transition moment may be obtained. Unfortunately the zero-field stationary states are coupled to one another in the presence of an electric field and the contributions due to the mixing of the states must be estimated. Using the matrix elements given by Oka,[6] matrices were obtained for the upper and lower levels of the respective transitions. Eigenvectors were generated by diagonalizing the matrices and were used to obtain the corrections to the observed transition moments. The result of these calculations along with an angular correction of $-2.5°$ to the attenuator yields three values, 0.201, 0.210, and 0.216 D corresponding to the $R(1,1)$, $Q(1,1)$, and $P(1,0)$ transitions, respectively, for the $\nu_3=1\leftarrow 0$ transition moment where the $-2.5°$ correction was determined by minimizing the spread in the above values. The transition moment derived from the $P(1,0)$ data is probably the more accurate of the three values since it depends the least on any zero corrections of the attenuator. The average value of the transition moment from the three values is therefore 0.21 ± 0.01 D, where the error reflects the angular correction of the polarizer used to minimize the spread. This value can be compared with transition moments estimated from data in the literature. Oka[17] has estimated the transition moment to be 0.144 D by using the absorption coefficient measurements of Hodges and Tucker.[18] Band-intensity data may also be used to estimate the transition moment. From the data of Kondo and Saëki[19] a value of 0.182 D is obtained, which is in better agreement with our result. It should be noted that Ref. 19 also contains a calculated value for the band intensity. Using this value, a transition moment of 0.195 D is obtained, which is in very good agreement with our result. A lifetime associated with the $\nu_3=1$ vibrational state may be calculated using the formula of Ref. 20,

$$\tau_s=\frac{\pi\epsilon_0 c^3\hbar}{\mu^2\omega_0^3}\ , \tag{7}$$

to be 21 ± 2 ms. In order to obtain the lifetime of a certain rovibrational transition, this value need only be divided by the square of the direction cosines for that transition.

The finite vertical spread of the molecular beam and the residual Doppler width due to horizontal divergence were found to have significant effects on the oscillations. It was found experimentally that without some collimation in front of the bolometer, Rabi oscillations of good contrast could not be obtained. The 350 μm slit in front of the bolometer was used to reduce the Doppler fullwidth to a calculated value of 160 kHz, which is less than the best observed $Q(1,1)$ FWHM of 215 kHz. The estimated vertical height of the molecular beam, $\simeq$2 mm, at the laser crossing also affected the bolometer signal. This effect produces a range of Rabi angles due to the Gaussian distribution of the laser-field amplitude. Although calculations based on the Bloch vector model were used to show that the vertical spread is an important source of damping, collimation was not used in this direction since the observed signal intensities would be further reduced

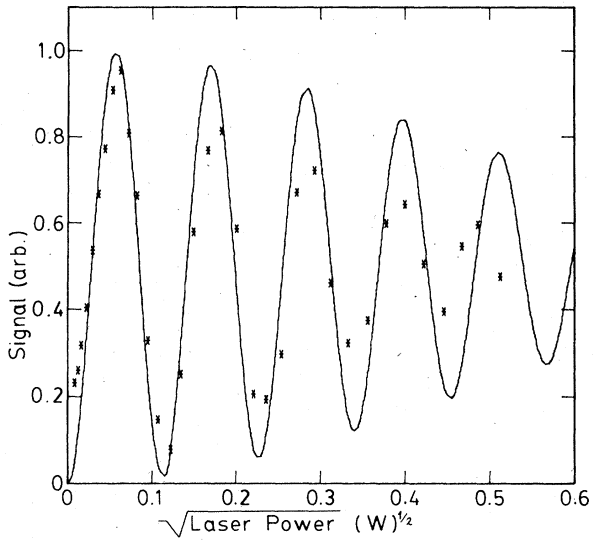

FIG. 5. $Q(1,1)-1\leftarrow 0$ Rabi oscillation data of Fig. 2(a) are superimposed on a Bloch-model simulation. The damping mechanisms used in the model are described in the text.

and an accurate determination of the transition moment could be made without this refinement.

The FWHM of the molecular speed distribution, $\simeq$6.5%, was also determined to be a damping factor. Calculations showed that this effect would reduce the amplitude of the Rabi oscillations by 10% over five oscillations. The data of Fig. 2(a) are scaled and superimposed upon a Bloch model curve in Fig. 5. All the effects discussed above are included in the model and the only adjusted parameter is the transition moment, which was obtained by the fitting procedure mentioned earlier. The figure shows that a large portion of damping is accounted for but that other damping effects are also present. One other source of damping may be laser jitter during the 4 μs molecular transit time but this was not included in the calculations since it could only be done in a phenomenological manner by assuming an exponential T_2 relaxation process in analogy with NMR.

As shown in the data of Fig. 2(b), it was found that the Rabi oscillations were not damped significantly even when the Gaussian laser waist was moved $\simeq$85 cm off the molecular beam. Wave-front curvature produces a frequency sweep as the molecules pass through the laser field. R-vector simulations incorporating this sweep yielded the progression shown in Fig. 6. As the distance from the waist increases, the Rabi oscillations are converted to rapid-passage processes leading to inversion at sufficient laser power. The damping mechanisms described above are included in these calculations and the calculations of Fig. 6(a) were chosen to have conditions similar to the data of Fig. 2(b). The effects of wave-front curvature have been described before in connection with the experiments on SF_6.[1] Those authors concluded that with their experimental arrangement, a slight change in location of the laser-beam waist with respect to the molecular beam caused rapid passage. The much greater displacement

needed in our experiment compared with the SF_6 experiment is presumably due to the much larger confocal parameter involved.

The contributions to the observed linewidths were described earlier in the experimental section. Assuming that these contributions are independent and add in quadrature then the total width can be written as

$$\Delta\nu=(\Delta\nu_T^2+\Delta\nu_D^2+\Delta\nu_E^2)^{1/2}\,, \tag{8}$$

where $\Delta\nu_T$ is the transit-time width, $\Delta\nu_D$ is the Doppler full width and $\Delta\nu_E$ is the width due to field inhomogeneities. Knowledge of the Stark-field tuning coefficient for the $Q(1,1)$ $-1\leftarrow 0$ transition[12] allows the spread of effective fields corresponding to a given $\Delta\nu_E$ to be calculated. Table I gives the $\Delta\nu_E$'s obtained for the linewidths measured for Figs. 2(a), 3(a), and 3(b) calculated by as-

TABLE I. Calculated electric field widths from Stark-field inhomogeneities.

Figure	$\Delta\nu$ (MHz)	$\Delta\nu_E$ (MHz)	θ (mrad)
2(a)	0.215	0	0
3(a)	0.232	0.087	0.033
3(b)	0.414	0.354	0.130

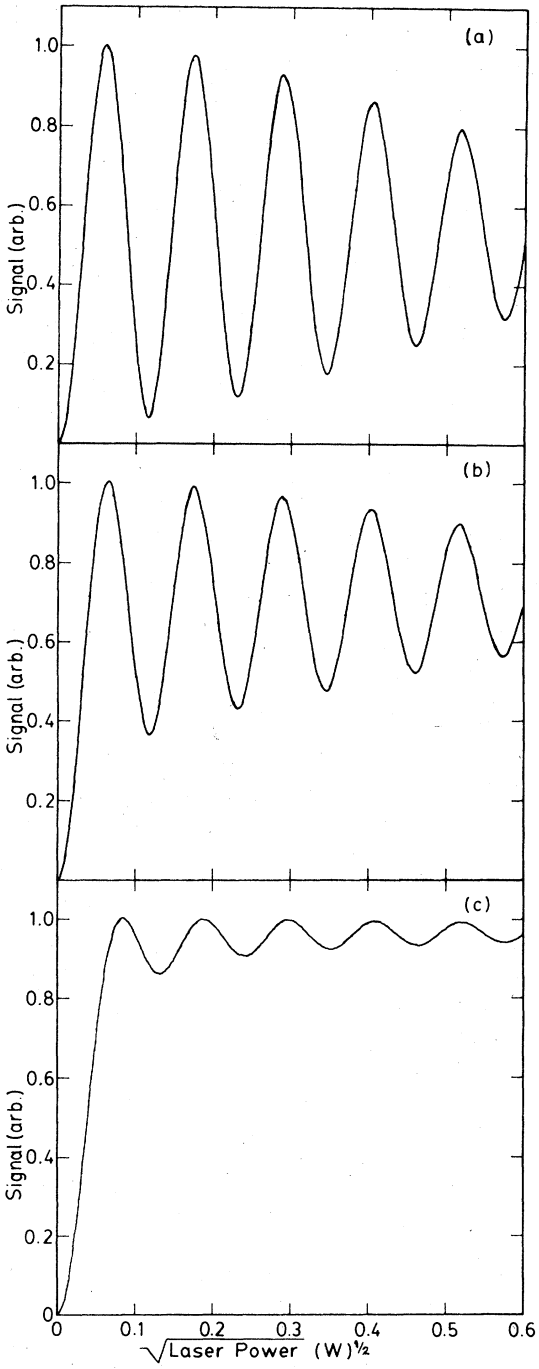

FIG. 6. Wave-front curvature effects were simulated using the Bloch model. (a)—(c) are simulations for distances of 0.78, 2.19, and 5.18 m from the laser waist, respectively. The Rabi oscillations are washed out and the system goes to inversion at higher laser powers when the waist is several meters off the molecular beam.

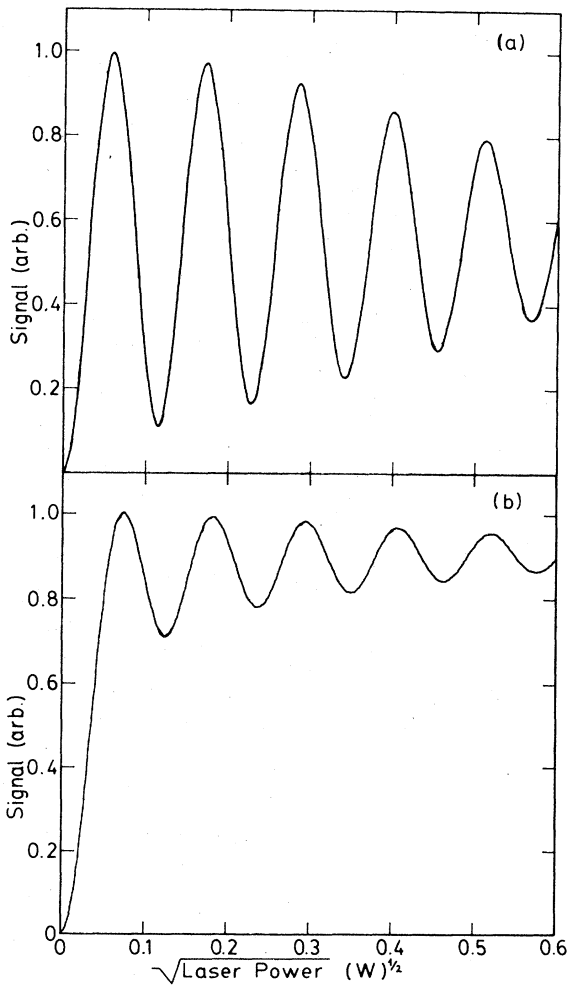

FIG. 7. Theoretical predictions for tilting of the Stark plate are shown. The conditions of Figs. 3(a) and 3(b) are used for (a) and (b), respectively.

suming that the data of Fig. 2(a) exhibited no electric field effects. From these values the tilt angle of the Stark plate was calculated for each case. This linear sweep of electric field seen by the molecule was used in the Bloch model. Figures 7(a) and 7(b) show the predictions for tilting the plate about the laser-beam axis with the linewidths of Figs. 3(a) and 3(b) including the discussed damping effects. Qualitative agreement is quite good and the calculations show that rapid-passage effects are again occurring due, this time, to the sweep in electric field.

CONCLUSIONS

We have demonstrated that well-defined Rabi oscillations can be achieved using laser Stark spectroscopy on a molecular beam provided that certain damping mechanisms can be controlled or eliminated. The oscillations have been modeled using the Bloch-equation formalism and various mechanisms that damp the oscillations have been simulated and good qualitative agreement with the experiment has been obtained. It has also been shown experimentally that frequency sweeps associated with Stark-field gradients can destroy Rabi oscillations and drive the molecules to inversion at sufficiently high laser power. This effect, as well as similar rapid-passage effects due to wave-front curvature, have been successfully modeled. The electric field inversion can be eliminated through careful alignment and adequate machining of the Stark electrodes while the wave-front curvature effect can be eliminated by allowing the laser beam to cross the molecular beam such that a Gaussian waist with plane wave fronts is seen by the molecules.

A powerful new tool has been developed to determine transition dipole moments in the infrared spectral region. These moments may be determined directly through the observation of Rabi oscillations. Values obtained from these measurements can be used to check band-intensity measurements and theoretical predictions of dipole moment derivatives and to provide the lifetimes of excited states. From the three transitions measured in this experiment, we have determined the transition dipole moment for the $\nu_3 = 1 \leftarrow 0$ vibrational transition of CH_3F to be 0.21 ± 0.01 D. The observed transition moment is in good agreement with values estimated from data in the literature.

ACKNOWLEDGMENTS

The authors would like to acknowledge funding of this project provided by the Natural Sciences and Engineering Research Council of Canada. One of us (A.G.A.) would also like to thank NSERC for financial support. Another of us (G.S.) would like to thank Franco Strumia for useful discussions.

[1]S. Avrillier, J. M. Raimond, Ch. J. Bordé, D. Bassi, and G. Scoles, Opt. Commun. **39**, 311 (1981).

[2]J. C. Berquist, S. A. Lee, and J. L. Hall, in *Laser Spectroscopy III,* edited by J. L. Hall and J. L. Carlsten (Springer, New York, 1977), p. 142.

[3]Ch. Salomon, Ch. Bréant, Ch. J. Bordé, and R. L. Barger, J. Phys. (Paris) Colloq. **42**, C8-3 (1981).

[4]J. E. Thomas, P. R. Hemmer, S. Ezekiel, C. C. Leiby, Jr., R. H. Picard, and C. R. Willis, Phys. Rev. Lett. **48**, 867 (1982).

[5]Ch. J. Bordé, Ch. Salomon, S. Avrillier, A. Van Lerberghe, Ch. Bréant, D. Bassi, and G. Scoles, Phys. Rev. A **30**, 1836 (1984).

[6]S. M. Freund, G. Duxbury, M. Römheld, J. T. Tiedje, and T. Oka, J. Mol. Spectrosc. **52**, 38 (1974).

[7]C. Douketis, T. E. Gough, G. Scoles, and H. Wang, J. Phys. Chem. **88**, 4484 (1984).

[8]M. Sargent III, M. O. Scully, and W. E. Lamb, Jr., *Laser Physics* (Addison-Wesley, Don Mills, Ontario, 1974), p. 91.

[9]R. L. Shoemaker, in *Laser and Coherence Spectroscopy,* edited by J. I. Steinfeld (Plenum, New York, 1978), p. 248.

[10]L. Allen and J. H. Eberly, *Optical Resonance and Two-Level Atoms* (Wiley, New York, 1975), p. 58.

[11]K. Shimoda, in *High-Resolution Laser Spectroscopy,* edited by K. Shimoda (Springer, New York, 1976), p. 14.

[12]R. H. Schwendeman (private communication).

[13]J. A. Harrison, Br. J. Appl. Phys. **18**, 1617 (1967).

[14]N. F. Ramsey, *Molecular Beams* (Oxford University, New York, 1956), p. 124.

[15]The confocal parameter is defined as $z_0 = \pi w_0^2/\lambda$, where w_0 is the minimum laser spot size and λ is the wavelength.

[16]C. H. Townes and A. L. Schawlow, *Microwave Spectroscopy* (McGraw-Hill, Toronto, 1955), p. 96.

[17]E. Arimondo and T. Oka, Phys. Rev. A **26**, 1494 (1982).

[18]D. T. Hodges and J. R. Tucker, Appl. Phys. Lett. **27**, 667 (1975).

[19]S. Kondo and S. Saëki, J. Chem. Phys. **76**, 809 (1982).

[20]K. Shimoda, in *High-Resolution Laser Spectroscopy,* edited by K. Shimoda (Springer, New York, 1976), p. 19.